# Ballistic gelatine—what we see and what we get

Christian Walter Albert Schyma, [1]✉

Email christian.schyma@irm.unibe.ch

[1] Institute of Forensic Medicine of the University of Bern, Bühlstr. 20, 3012 Bern, Switzerland

Received: 15 August 2019 / Accepted: 7 October 2019

# Abstract

Since decades, 10% gelatine is used to visualize and estimate the energy transfer of projectiles. The study performed investigates the correlation of the temporary cavity (TC) recorded by high-speed video (HSV) and the cracks in gelatine slices. A total of 36 shots were performed from distance using form-stable bullets (FMJ), 12 using deforming bullets (HP) in the calibres .32 auto, .38 special and 9 mm Luger. The target models were prepared according to Fackler's standard as 10% gelatine cubes with 12 cm edge length doped with a paint pad beneath the front cover ("reference cube"). Scaled images of the TC were recorded with 40.000 fps. The cubes were cut into 1-cm-thick gelatine cross sections, which were scanned. The evaluation of the destruction (cracks) was performed by the mean of image analysis measuring the longest crack, the wound profile according to Fackler and applying the polygon method. The height of the TC was measured each cm along the bullet path. The energy deposited ranged between 54 and 269 J. FMJ caused tubular, HP provoked pear-like TC. The tubular aspect was consistent with the quasi-constant deceleration of FMJ; however, the pear-like TC did not metrically represent the deceleration of HP. The profiles of destruction parameters were convex for both projectile types and did not match the profile of bullet deceleration. The maximum of TC stretching observed in HSV did not coincide with maximum gelatine destruction (crack lengths). The total energy transfer correlated with all considered destruction parameters in their sum; however, the cross-sectional parameters did not reflect the energy transfer per centimetre bullet path. The sum of the TC's heights correlated with the energy deposited, but differently for FMJ and HP. Obviously, the 12-cm reference cube reflects the energy transfer by a bullet as a whole.



## Keywords

Wound ballistics
Simulants
Temporary cavity
High-speed video
Energy transfer

# Introduction

AQ1

Gelatine is used as a simulant in wound ballistic research since decades [1]. The preparation of gelatine is rather standardized [2, 3, 4, 5, 6] using type A gelatine with a gel strength of 250 to 300 Bloom. Fackler and Malinowski introduced 10% gelatine at 4 °C as a standard while NATO specification provides 20% gelatine at 10 °C [1]. The main qualities of gelatine are the elasticity and the transparency. The first makes the simulant interesting for the comparison with biological tissues; the second is advantageous for visualizing the bullet simulant interaction, especially by the mean of high-speed video recording. When a projectile passes through gelatine, it is decelerated and the lost kinetic energy is deposited in the simulant. Gelatine is accelerated and displaced perpendicularly to the bullet path, so that a cavity visible for few milliseconds is formed, which collapses due to the elastic property of the gelatine in a damped oscillation. This phenomenon is called the temporary cavity (TC). Its volume is proportional to the energy transferred [1]. After shooting, the gelatine blocks are cut into slices perpendicularly to the bullet path. In the slices, radial cracks are observed as remains of the TC. The evaluation of the visible alteration can be performed measuring all the crack lengths per slice (total crack length method TCL [1, 7, 8]), the two largest cracks per slice (Fackler's wound profile [9]) or drawing a polygon by linking the ends of the cracks (polygon perimeter and area [10]). The integral of each destruction parameter over the gelatine block is proportional to the energy transferred in the whole block [11].

In consequence, it should be possible to correlate also the size of the TC estimated from high-speed video (HSV) with the totalized destruction parameters.

# Methods

A total of 48 experimental shots on gelatine blocks under standardized conditions (10% gelatine "Ballistic III", 4 °C, storage for at least 48 h [11]) from distance had been performed using full metal jacketed ($n$ = 36) and deforming bullets ($n$ = 12) fired from common handguns in forensically relevant calibres (.32 auto, .38 special, 9 mm Luger). The shots were recorded using a SA-X2 high-speed camera (Photron Europe Ltd., West Wycombe, UK) with 40,000 fps perpendicularly to the direction of fire. The target velocity (before penetration) and the rest velocity (behind the target) of the bullet were calculated from high-speed video (HSV) as published previously [12, 13].

HSV sequences were evaluated to identify the frame, which shows the end of the TC expansion phase. In this frame, the gelatine cube was overlaid by a 12-line grid allowing for perpendicular measurements of the TC's height (Fig. 1). Gelatine blocks were cut perpendicularly to the bullet path into 1-cm-thick slices which were scanned at 300 dpi [10]. Cross-sectional analysis considered the wound profile (WP) according to Fackler [9], the polygon perimeter (PP), the polygon area (PA) and the maximum crack length ($R_{max}$) [11]. The less reproducible TCL was not applied. Axio Vision 4.9 64 SE (Zeiss, Oberkochen, Germany) was used to perform measurements on scaled images of scanned gelatine slices and video frames. The data were analysed using Excel (Microsoft, Redmond, USA).

**Fig. 1**

Frame 0.7 ms after penetration of a 9- mm Luger FMJ bullet, which left a tubular temporary cavity (159 J energy deposited). The 12-line grid serves for measuring the height of the TC

AQ2

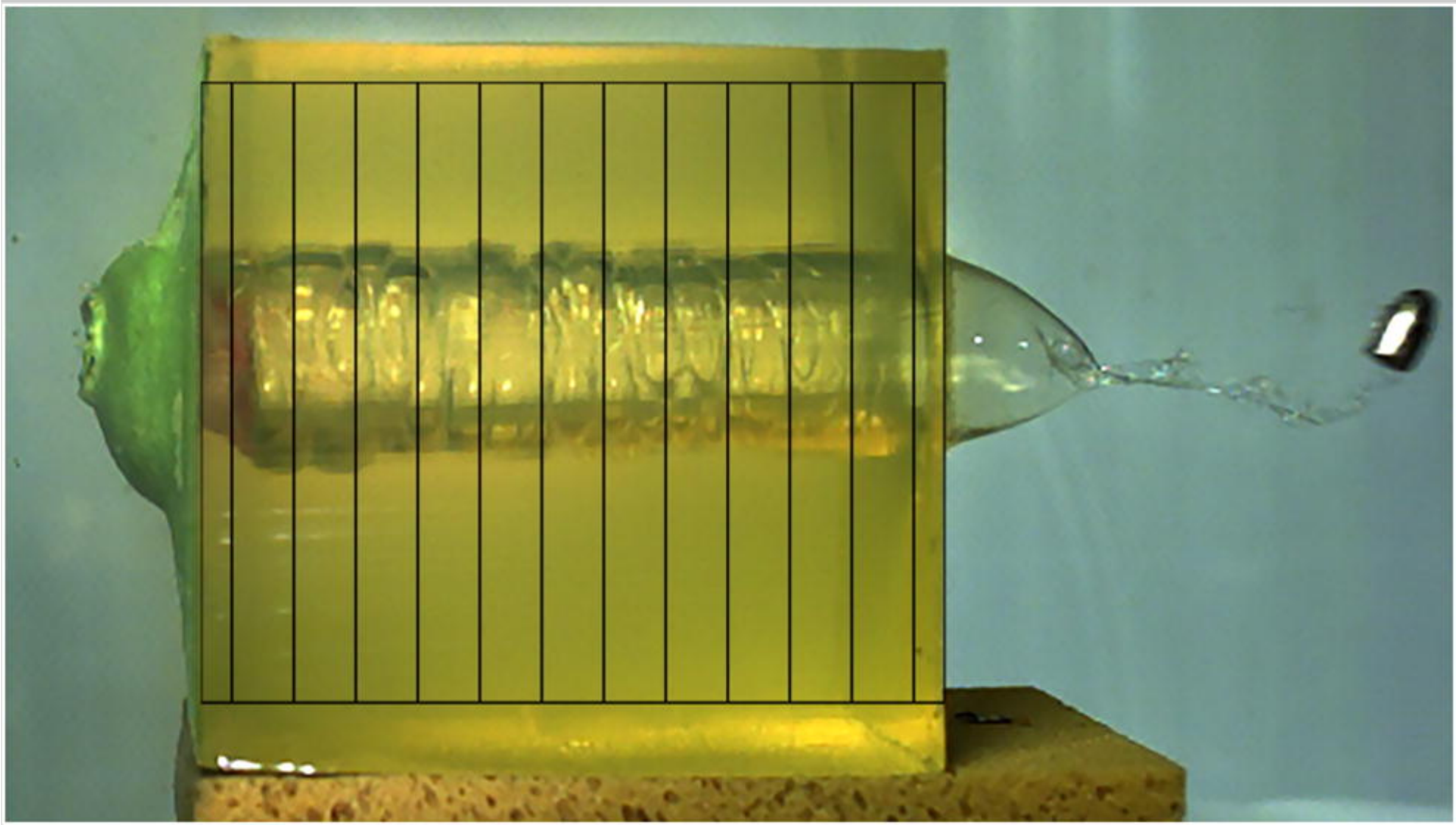

## Results

In all experimental shots, the colour contrast method [10] was used to enhance the visibility and stability of cracks in gelatine. The presented study considers exclusively 12-cm-long blocks with 12 cm height and 12 cm width [14], which

were put on a sponge as elastic underlay to allow for an unrestricted expansion of the TC [15]. All bullets perforated the target model. FMJ bullets ($n$ = 36, 12 per calibre .32 auto, .38 special and 9- mm Luger) remained intact, whereas all deforming bullets ($n$ = 12, hollow point ammunition, HP) were found fully expanded without fragmentation or separation of core and jacket. The reproducibility of measurements in HSV frames as well as in scanned images was repeatedly controlled for more than 12 months and found typically better than 0.5%.

## High-speed video

In high-speed video (HSV), two principally different forms of the TC were distinguished. Form stable projectiles (FMJ) caused a tubular shaped TC, independently of the shape of the projectile nose (round or ogival). The height ($H$) of the TC was practically equal all over the bullet path and varied for each shot in correlation to the energy deposited (54 to 159 J). The analysis of the TC's relative height ($H_i$ / $\sum_{i=1}^{12} H_i$) showed perfectly matching flat curves for all three calibres (.32 auto, .38 special, 9 mm Luger) (Fig. 2).

**Fig. 2**

Profiles of FMJ bullets ($n$ = 12 per calibre). Above the relative heights of the TC, below the polygon perimeter PP as an example ($R_{max}$ and WP showed the same form)

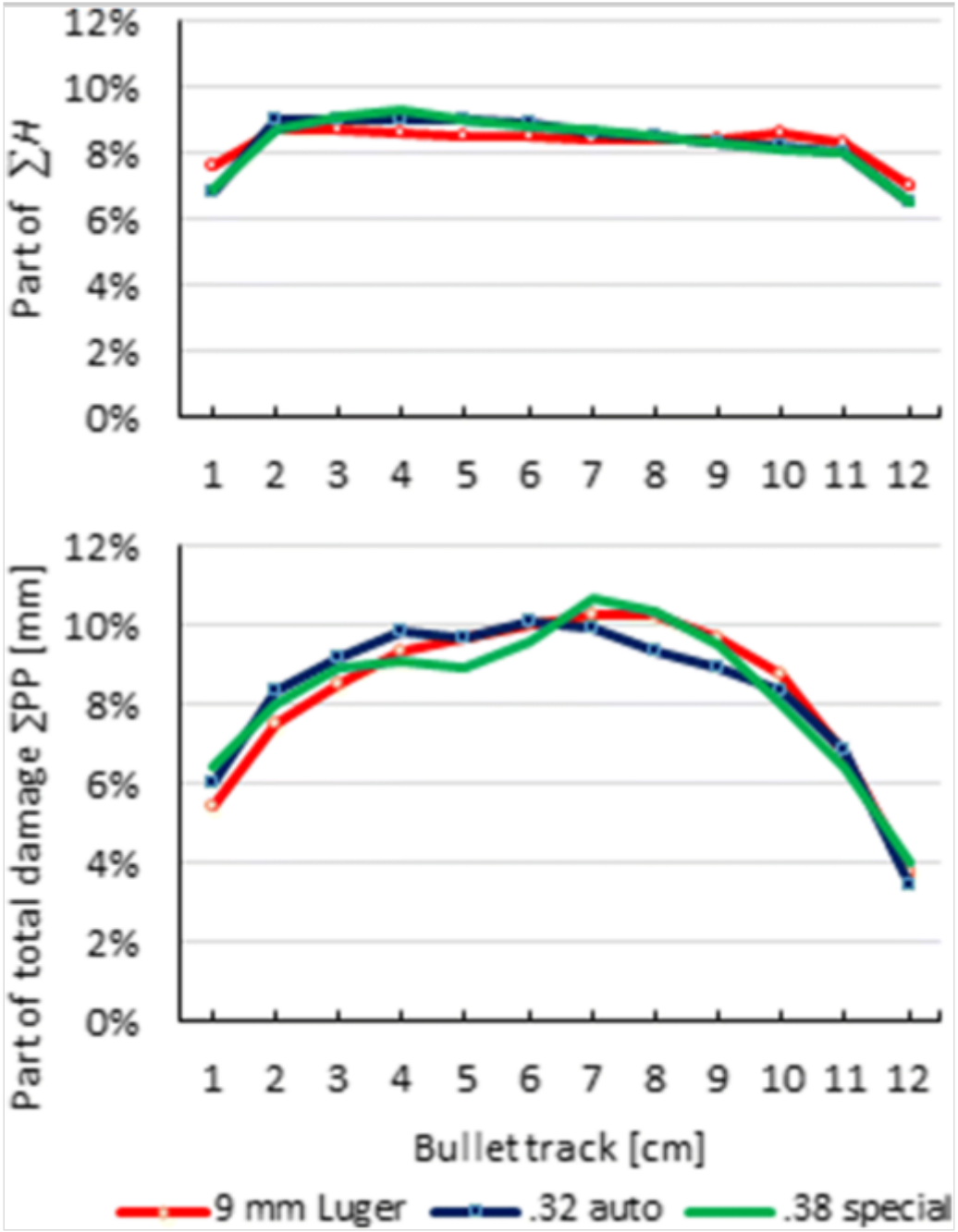
12%
10%
8%
6%
4%
2%
0%
Part of ∑H
1 2 3 4 5 6 7 8 9 10 11 12
12%
10%
8%
6%
4%
2%
0%
Part of total damage ∑PP [mm]
1 2 3 4 5 6 7 8 9 10 11 12
Bullet track [cm]
9 mm Luger
.32 auto
.38 special

Deforming bullets (HP) in the calibre .32 auto produced an asymmetric TC with a higher expansion of the TC in first third of the bullet path and a conical diminution in the last two thirds. The resulting form remembered a pear and was roughly similar for the ammunition brands. The energy transferred ranged between 140 and 162 J. The point of the maximum height was reached after 3- to 4- cm bullet path by Silvertip (Winchester, East Alton, USA) (Fig. 3) and Gold Dot (Speer CCI Ammunition, Lewiston ID, USA), after 4 to 5 cm by the Guardian Gold bullet (Magtech Lino Lakes, USA) (Fig. 4).

**Fig. 3**

Frame 1.625 ms after impact of a .32 auto Silvertip hollow point bullet. Pear-like form of the TC at the end of its expansion phase. Energy deposited 140 J

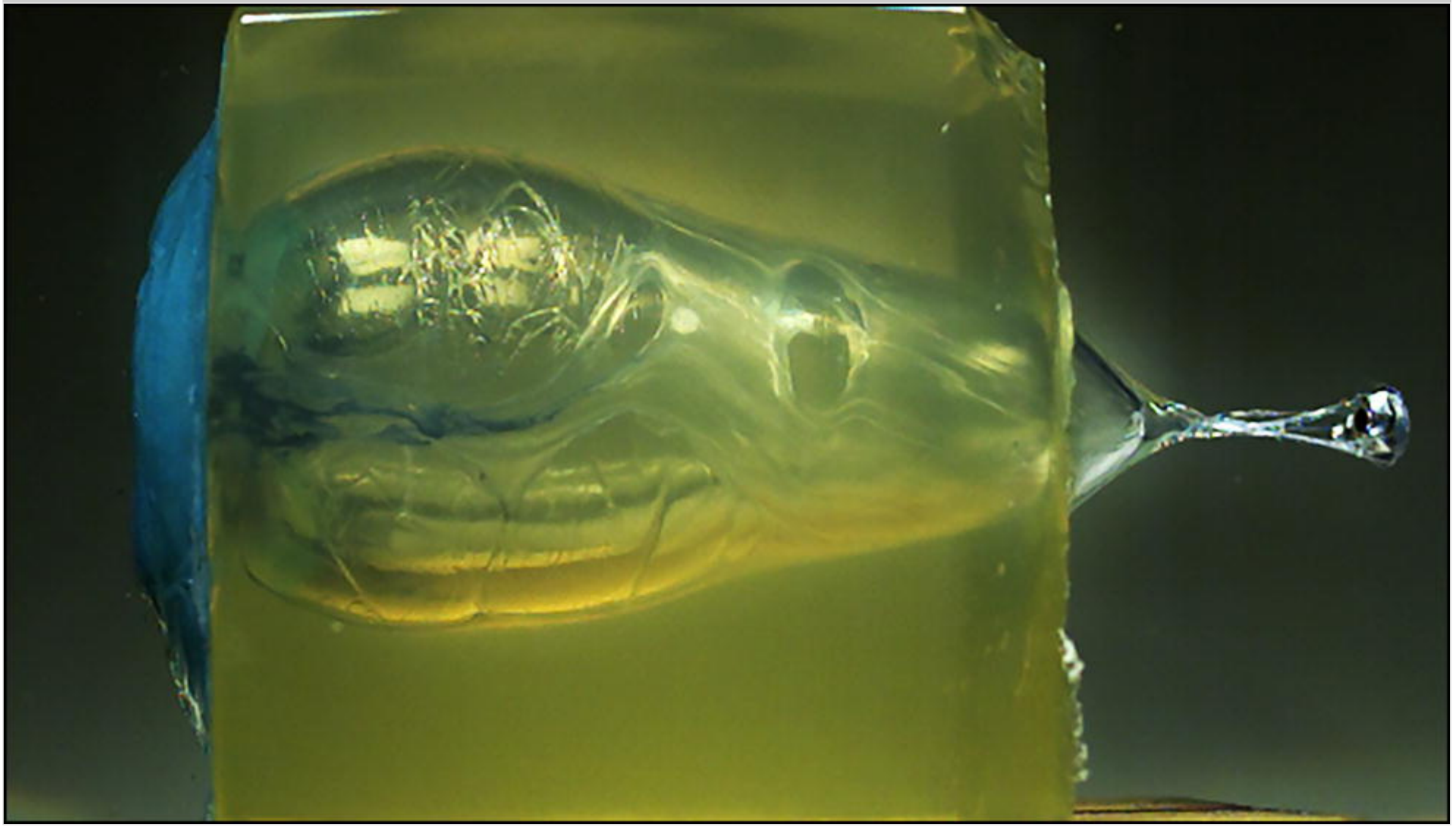

**Fig. 4**

More elongated TC caused by a .32 auto GuardianGold deforming bullet which delivered 157 J

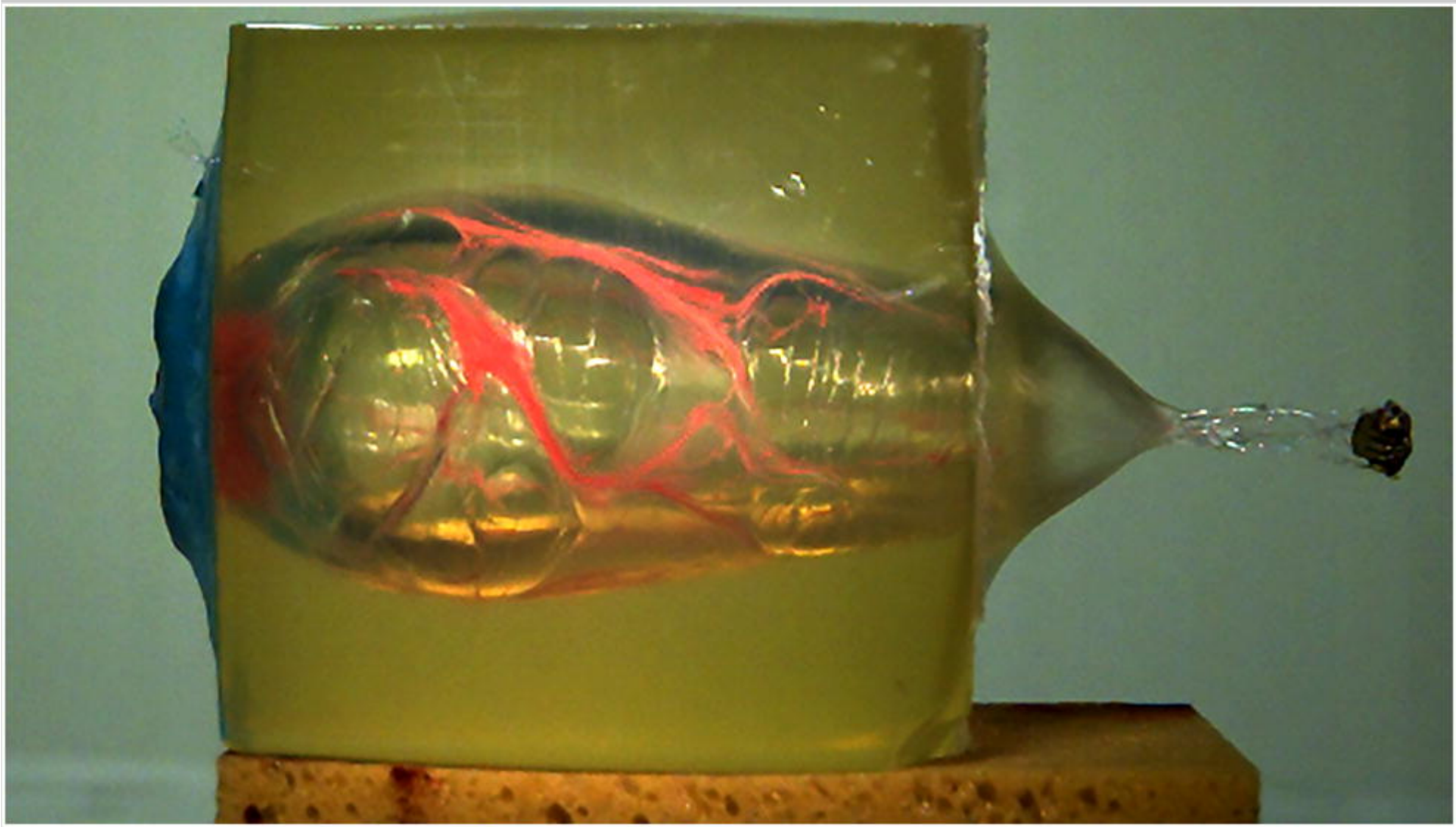

When firing .38 special expanding bullets, the energy deposited was higher (232–269 J) and the pear-like form could only be observed in the early phase of TC expansion. Later on, before the maximum of the TC was reached, this initial

asymmetric shape transformed more and more into a rather symmetric ball stretching the gelatine cube in all directions (Fig. 5). The vertex of the expanded TC was noted at 4- to 5- cm bullet path.

**Fig. 5**

Evolution of the TC caused by a .38 special deforming bullet (energy deposited 262 J). Left frame (1.7 ms after impact) shows the end of the TC's expansion phase and right frame 1.1 ms later (2.8 ms after impact) with maximal ballooning during collapse

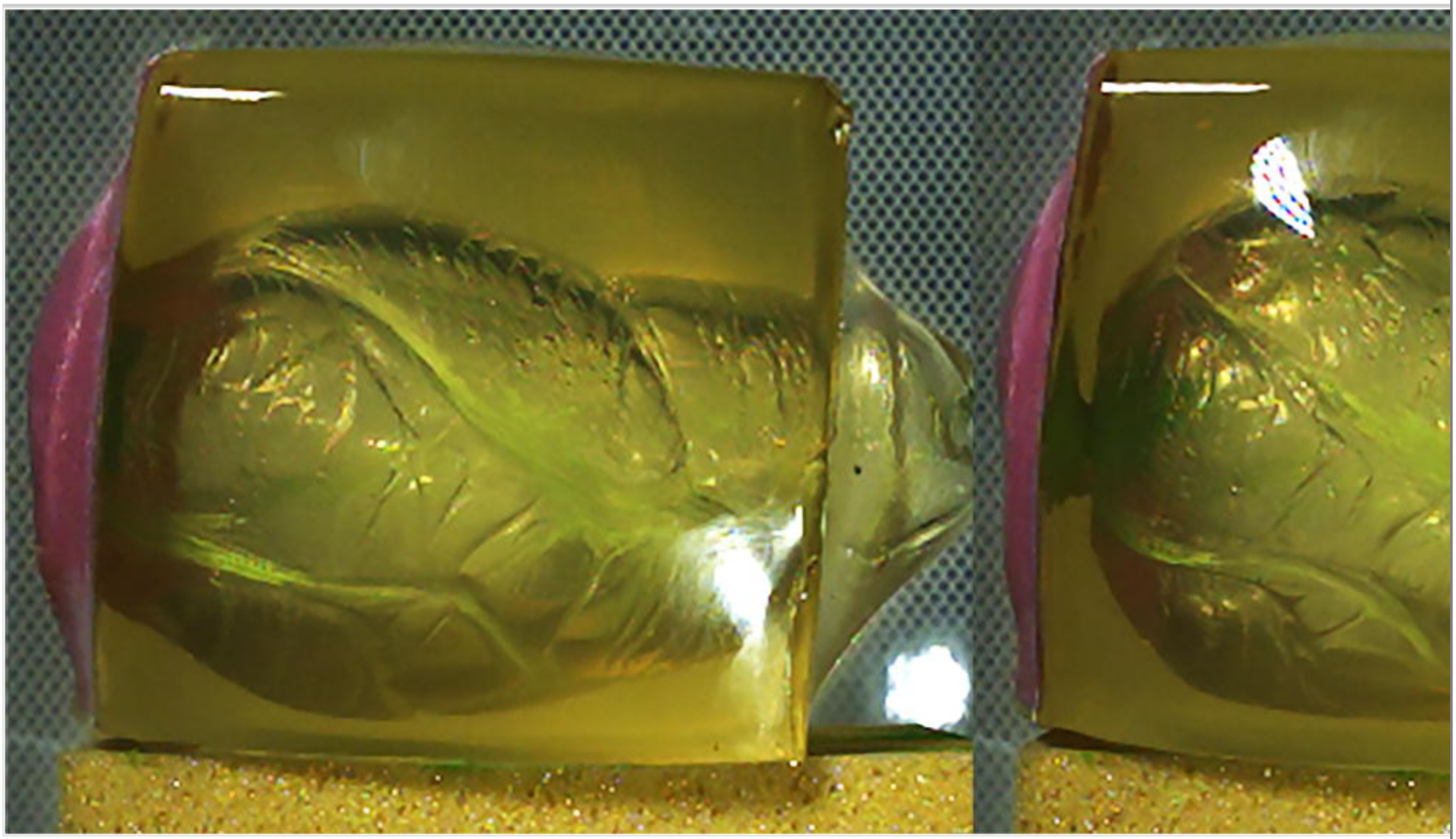

Damage in gelatine cross sections

The profiles of the cross-sectional analysis showed for the majority of projectiles a rather symmetric convex curve independently from the parameter of destruction (WP, PP, PA, $R_{max}$). Only deforming .32 auto ammunition tended to an asymmetric profile. In order to compare different parameters and to be independent from the absolute energy transferred, the partial damage for each slice was calculated as percentage of the added up destruction parameter over all 12 slices ($x_i$ / $\sum_{i=1}^{12} x_i$).

For FMJ bullets, a significant difference was not observed. The polygon perimeter PP (Fig. 2) matched the curves of the wound profile and the longest crack ($R_{max}$). The curve of the polygon area was always more convex and in most of the FMJ shots irregular. Looking at the 9- mm Luger shots ($n$ = 12) as an example, the relative smooth profile of PP, WP and $R_{max}$ graphs is statistically supported by a low part of damage which was randomly distributed above the convex curve of minimal damage: PP 11.7%, WP 12.5% and $R_{max}$ 14%. Hence, all individual curves were situated in a small corridor. In contrast, the polygon area was varying for 25.9% of the total damage. Summarizing, in the mean, the maximum damage was observed at 6- to 8- cm bullet path for all parameters.

Deforming bullets showed a maximum of damage after 4 to 6 cm penetration depth (.32 auto) respectively at 5 to 7 cm (.38 special) (Fig. 6). The Silvertip (cal. .32 auto) deposited only 140 J but showed the most skew profile with maximum at 4 cm. The kurtosis of the graphs was always higher for expanding bullets than for FMJ. When the parameters were separately analysed for the five shots .32 auto Gold Dot (Fig. 7) and the four shots .38 special First Defense (Magtech Lino Lakes, USA), the variation above the minimum curve was less than for the FMJ: PP 6–8%, WP 8–9%, $R_{max}$ 12–13%, PA 9% (.38 special) and 17% (.32 auto). This difference might be explained by a relatively better measuring accuracy with respect to the higher values caused by higher energy deposit. The remarkable fitting of the PA curves for the powerful deforming bullets is underlining the hypothesis.

**Fig. 6**

Fackler's wound profile as partial damage along the bullet track. The skewer curve of .32 auto Gold Dot (GD) in comparison with the rather symmetric curve for .38 special deforming First Defense (FD) and the flatter line for 9- mm Luger FMJ

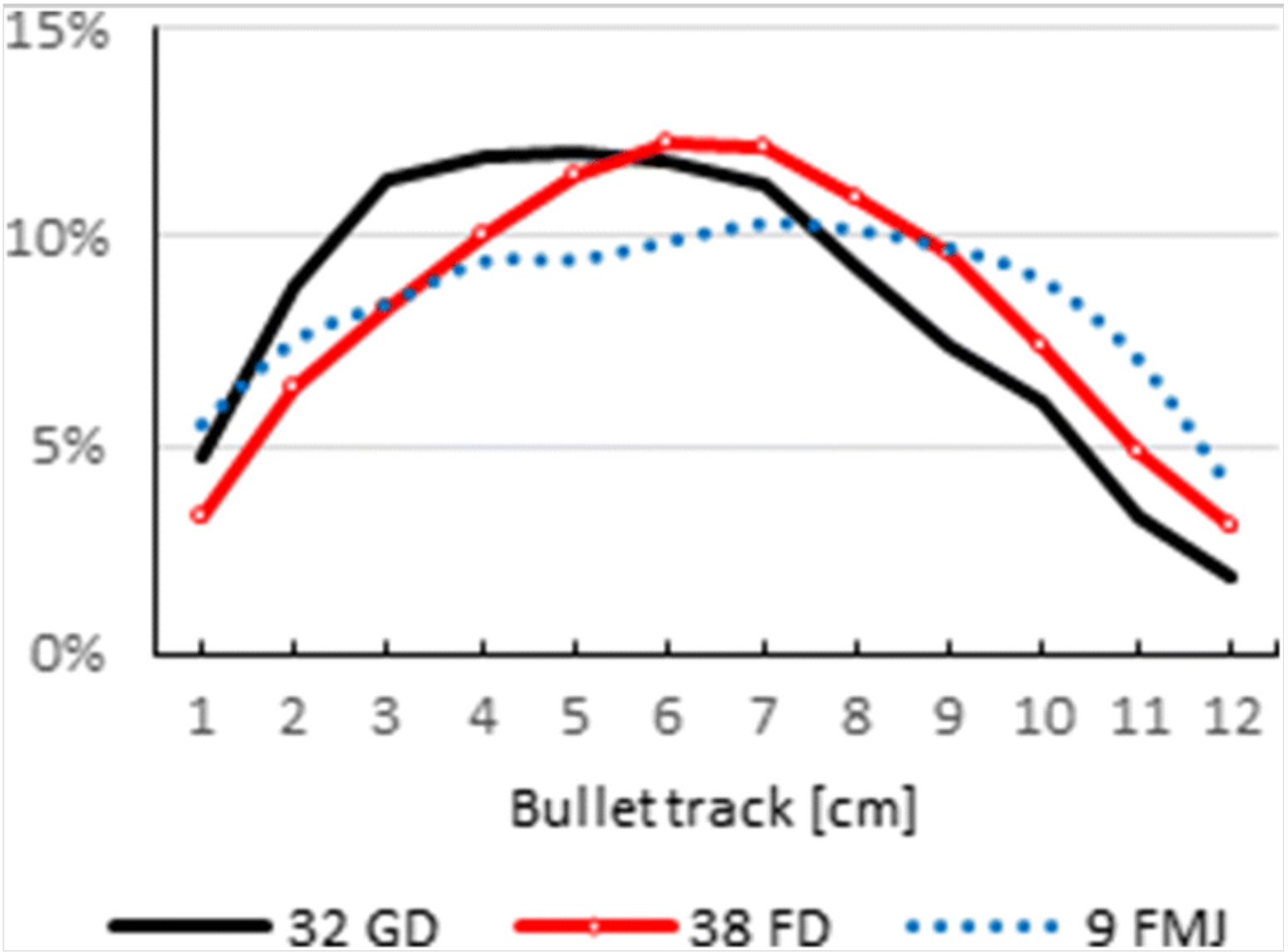


**Fig. 7**

Mean values of .32 auto Gold Dot ($n$ = 5). The mismatch of the TC's height with the destruction parameters in cross sections is obvious. WP and $R_{max}$ are not displayed because they matched perfectly the graph of PP. PA polygon area, PA-2 √PA, PP

polygon perimeter, TC height of the TC from HSV

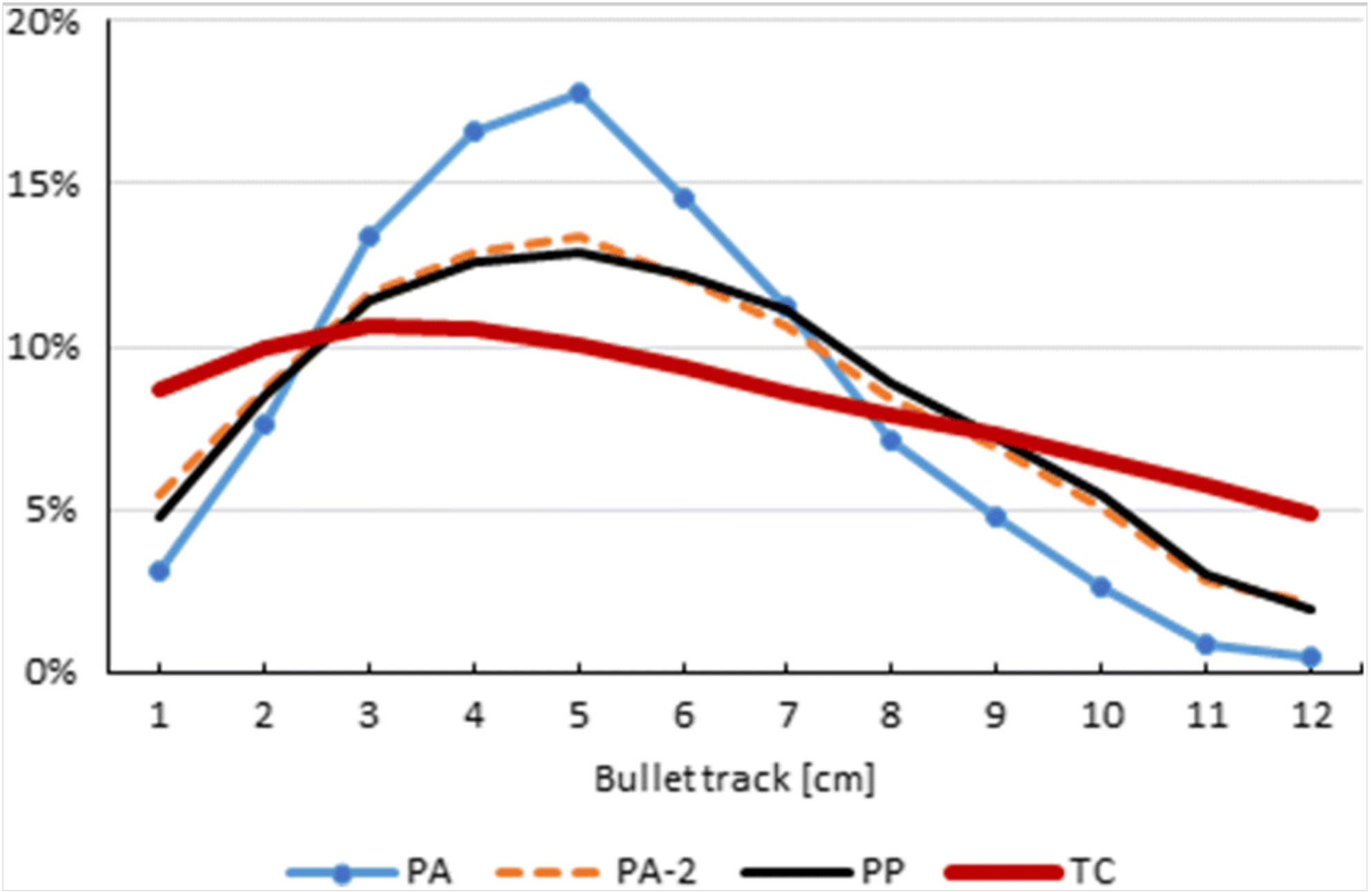

## Correlation analysis

The assumed linear correlation of energy deposited and the added up measurements in a block (heights of the TC in HSV and the destruction parameters in cross sections) was investigated.

The coefficient of determination ($r^2$) for linear regression is displayed in Table 1. The regression lines for length parameters obtained from gelatine slices (PP, WP, $R_{max}$) were practically identical for FMJ and HP (Fig. 8). The regression for the polygon area PA caused regression lines with different slopes for FMJ (lower energy transfer) and HP bullets. When instead of PA its square root $\sum \sqrt{}$ PA was totalized, a single regression line for FMJ and HP was obtained. However, the correlation of the $\sum H$ (sum of heights) with the energy transferred resulted in two different regression lines with similar slope (Fig. 9) for both types of projectile. All parameters showed a wider scattering in shots with low-energy transfer.

**Table 1**

Coefficient of determination ($r^2$) for linear correlation of total energy transferred and the totalized parameters

AQ3

| Parameter | $\sum H$ | | $\sum$PA | | $\sum \sqrt{}$ PA | $\sum$PP | $\sum$WP | $\sum R_{max}$ |
|---|---|---|---|---|---|---|---|---|
| | FMJ | HP | FMJ | HP | | | | |
| $r^2$ | .850 | .933 | .649 | .919 | .845 | .833 | .847 | .868 |

*H* height of the TC, *PA* polygon area, *PP* polygon perimeter, *WP* Fackler's wound profile, $R_{max}$ maximum crack length, *FMJ* full metal jacketed bullet, *HP* deforming bullet

**Fig. 8**

Correlation of the cumulated polygon perimeter with the energy deposited. HP deforming bullets

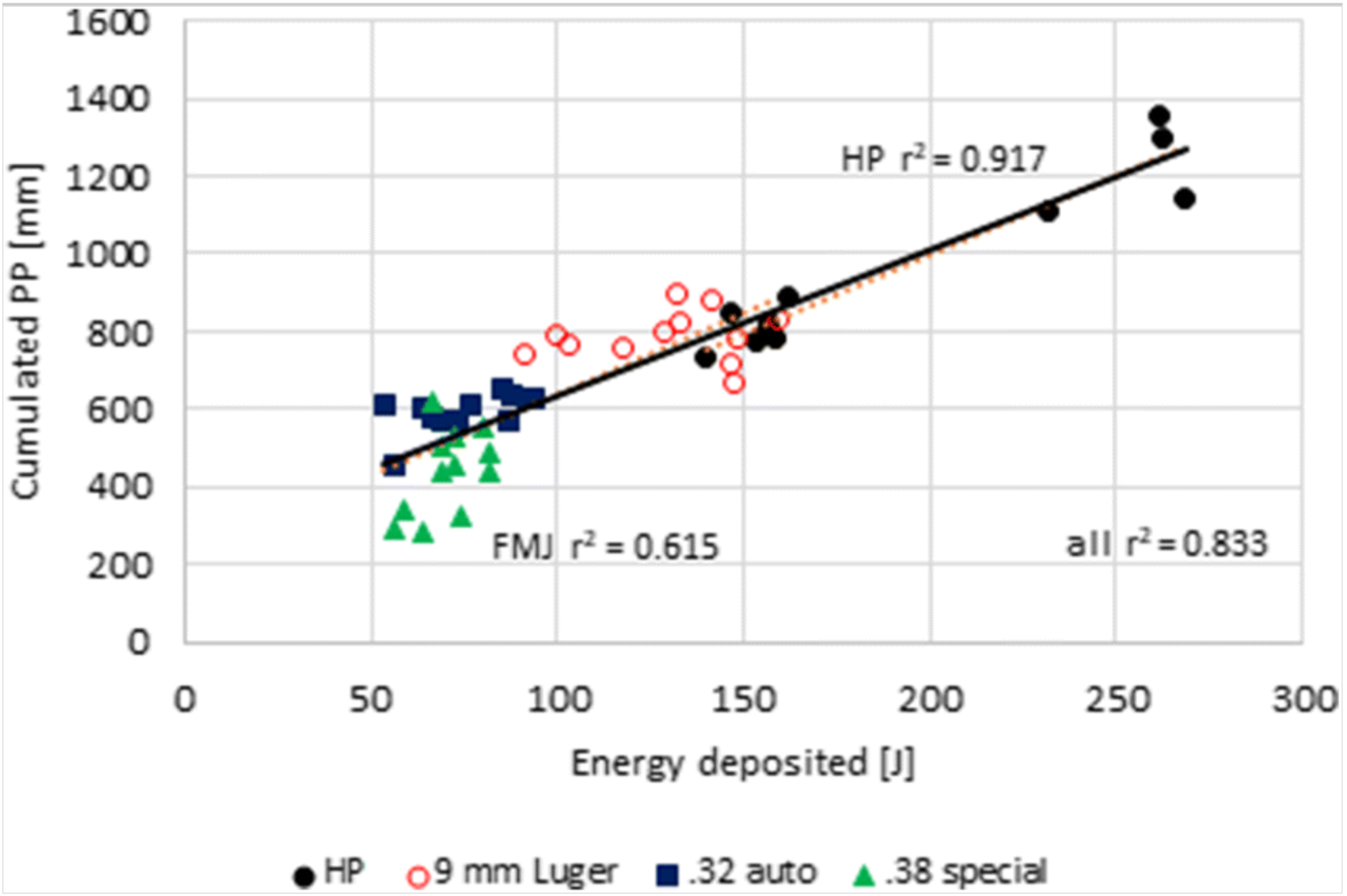
1600
1400
1200
1000
800
600
400
200
0
Cumulated PP [mm]
HP r² = 0.917
FMJ r² = 0.615
all r² = 0.833
0
50
100
150
200
250
300
Energy deposited [J]
HP
9 mm Luger
.32 auto
.38 special

**Fig. 9**

Correlation of the cumulated heights of TC with the energy deposited. HP deforming bullets

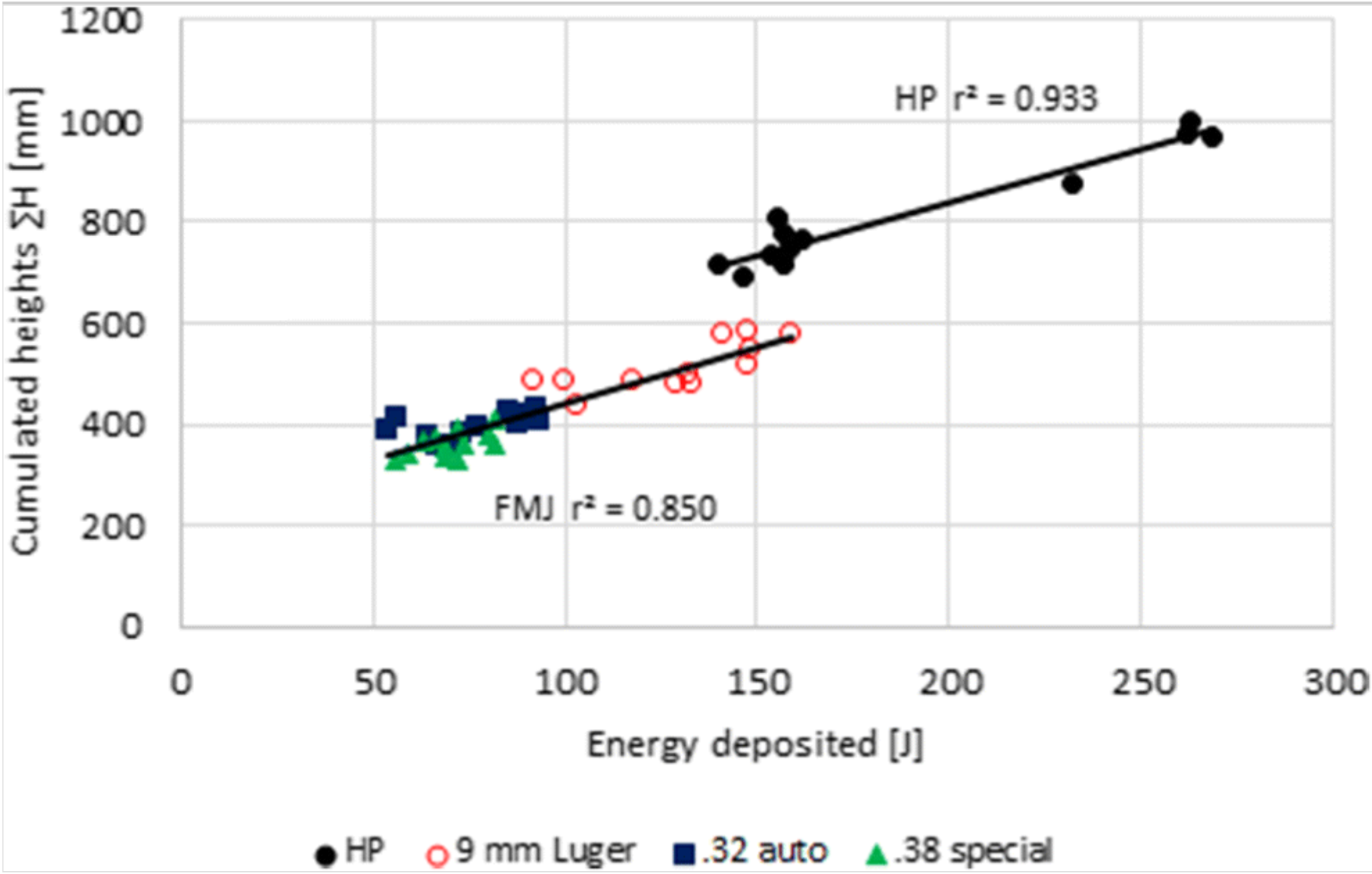
Cumulated heights ΣH [mm]
1200
1000
800
600
400
200
0
0
50
100
150
200
250
300
Energy deposited [J]
HP r² = 0.933
FMJ r² = 0.850
HP
9 mm Luger
.32 auto
.38 special

Further, the interdependence of all parameters was tested. To perform correctly linear correlation analysis, only one-dimensional parameters (mm) were considered. Therefore, PA was substituted by its square root. Table 2 shows the strong interdependence of all parameters obtained from cross-sectional analysis ($R_{max}$, WP, PP and $\sqrt{PA}$). The height of TC ($H$) in HSV as a methodically independent measurement is rather good correlating with the other destruction parameters when the energy transfer is sufficient ($r^2 > 0.8$ for deforming bullets HP).

**Table 2**

Coefficient of determination for linear correlation of the totalized parameters among each other. The right upper half displays $r^2$ for FMJ, the left lower half for deforming bullets. (Abbreviations given in Table 1)

| **FMJ HP** | $\sum H$ | $\sum R_{max}$ | $\sum WP$ | $\sum PP$ | $\sum \sqrt{PA}$ |
|---|---|---|---|---|---|
| $\sum H$ | | 0.711 | 0.684 | 0.652 | 0.652 |
| $\sum R_{max}$ | 0.805 | | 0.975 | 0.940 | 0.813 |
| $\sum WP$ | 0.811 | 0.975 | | 0.984 | 0.918 |
| $\sum PP$ | 0.857 | 0.940 | 0.984 | | 0.988 |
| $\sum \sqrt{PA}$ | 0.862 | 0.922 | 0.953 | 0.988 | |

# Discussion

*Ex nihilo nihil fit* (nothing comes from nothing). This classical proverb is quasi the base of wound ballistics. In other words, each injury requires an acting force and therefore only the energy delivered by a bullet has the potential to wound. Hence, in penetrating or perforating gunshot injuries, the local energy transfer is the most important aspect to be investigated [1]. The common approach in wound ballistics is to describe the energy transfer of projectiles in surrogates (gelatine, glycerine soap, clay) which are—simplifying the reality—called (tissue) simulants. In simulants with plastic behaviour (soap, clay), the bullet provokes a cavity whose volume represents the energy delivered. In elastic gelatine,

however, the cavity induced by radial displacement of the medium is collapsing after only few milliseconds; wherefore, the cavity is called temporary and in consequence has vanished after shooting. Nevertheless, there are three ways to estimate the energy transferred.

- Due to the transparency of gelatine, it is possible to record the formation of the TC during shooting using HSV. In so doing, we have at least a two-dimensional image of the TC, which can be sized.
- Using HSV with short exposure times (2.5 µs or less), the deceleration of the bullet can be calculated [13].
- Cross sections of gelatine blocks show the cracks which remain after the TC's collapse.

The presented study was conducted using the reference cube, a 12-cm-long gelatine cube. As expected, the shape of the TC was clearly different for non-deforming and deforming bullets.

FMJ bullets, which were form-stable, produced a tubular shaped TC independently of the calibre or the energy. This was consistent with the findings of the previously measured deceleration of these bullets which showed a constant loss of velocity [13]. Surprisingly, none of the destruction parameters evaluated in gelatine sections did match this profile. All parameters showed a relatively symmetric convex profile instead of a straight horizontal line. No matter which parameter was chosen, the maximum of damage was observed at 6 to 8 cm penetration depth, which points approximatively at the middle of the target model. Optically, this finding was corresponding with the region where the first collapse of the TC took place.

Deforming bullets produced a TC, which was always clearly different from that caused by FMJ bullets. However, the pear-like form of the TC did not match the profile of the deceleration published previously [13]. According to the cited previous study and literature [1, 16], the deformation of handgun hollow point bullets occurs within the first 2 cm of the bullet path in gelatine corresponding to an abrupt deceleration. The subsequent deceleration of the deformed bullet is rather constant similar to form-stable projectiles. This observation would implicate a much higher energy transfer in the first 2 cm of the bullet path. However, the TC shows the maximal height only between 3 and 5 cm penetration depth depending on the ammunition brand and kinetic energy. Generally spoken, the higher the kinetic energy of the hollow point bullet, the more

symmetric is the resulting balloon-like form of the TC. Cross-sectional analysis of the gelatine slices confirms this observation. Weaker deformation bullets show a skewer, asymmetric profile of damage with focus in the first half of the bullet path (maximum between 4 and 6 cm for calibre .32). Projectiles delivering more energy, such as .38 special HP bullets, cause rather symmetric convex curves (maximum at 5 to 7 cm) similar to those described for FMJ, but steeper.

The results remembered published observations where head models had been used [14, 15, 17, 18, 19, 20].

Particularly, because the damage profile in gelatine did not reflect the expected energy transfer, the question remained open, if there is any correlation of cracks in gelatine and deposited energy. This issue had already been addressed by Ragsdale et al. [8, 21]. Adding up each destruction parameter over all twelve slices of the gelatine block, the resulting sum correlated closely to the total energy transferred $E_{\text{deposited}} = E_{\text{initial}} - E_{\text{rest}}$. The correlation was linear for all one-dimensional parameters measured in gelatine cross sections. There were no qualitative differences between the parameters, the longest crack ($R_{\text{max}}$), the two longest cracks (WP, wound profile according to Fackler) or the polygon perimeter (PP). The relation between the polygon area (PA) and the energy deposited fitted best a power function. Actually, the square root $\sqrt{\text{PA}}$ correlated as well linearly as $R_{\text{max}}$, WP or PP.

In analogy to the cross-sectional analysis, twelve heights of the TC were measured in HSV frames. The sum of the heights $\sum H$ correlated closely in a linear function with the energy deposited when form-stable and deforming bullets were analysed separately. The reason is not clear why different linear regression lines resulted for both bullet types. This issue is notable because FMJ bullets with the same energy transfer as deforming bullets produced a significantly smaller TC.

As expected, all considered parameters were interdependent. Only when we regard the integral of a destruction parameter, we get a correlation with the energy transferred. This means summarizing that the gelatine cube reacts as a whole on the energy transfer. The probable reason might be the elasticity of gelatine.

What are the consequences of these observations? Longer and larger gelatine blocks like those that are currently used to get profiles of complete energy transfer [1] do not solve the problem to simulate a head. Another approach could be the search for a brain simulant with higher biofidelity [22, 23, 24, 25]. However, we could as well take into consideration that the head struck by a bullet might also react as a whole.

# Conclusion

The study is based on 12-cm-long gelatine cubes, which are used as surrogate to simulate gunshots to the head. The experimental shots using form-stable (FMJ) and deforming (HP) bullets were analysed based on high-speed video of the temporary cavity (TC) and cross-sectional examination in gelatine slices.

- FMJ cause tubular, HP provoke pear-like TC.
- The tubular aspect is consistent with the quasi-constant deceleration of FMJ.
- The pear-like TC does not metrically represent the deceleration of HP.
- The profiles of destruction parameters are convex for both projectile types and do not match the profile of bullet deceleration (continuous energy transfer).
- The maximum of TC stretching observed in HSV does not coincide with maximum gelatine destruction (crack lengths).
- The findings could be a first indication that the cracks in gelatine are not (only) determined by stretching but by the collapse of the temporary cavity.
- The total energy transfer correlates with all considered destruction parameters in their sum; however, the cross-sectional parameters do not reflect the energy transfer per centimetre bullet path.
- Also, the sum of the TC’s heights correlates with the energy deposited, but differently for FMJ and HP.
- The reference cube (12 cm edge length, 10% gelatine, 4 °C) reflects the energy transfer by a bullet as a whole.

## Publisher’s note

Compliance with ethical standards

*Conflict of interest* The author declares that he has no conflict of interest.

# References

1. Kneubuehl BP (2011) Simulants. In: Kneubuehl B (ed) Wound ballistics: basics and applications. Springer, Berlin Heidelberg, pp 136–143

2. Fackler ML, Surinchak JS, Malinowski JA, Bowen RE (1984) Bullet fragmentation: a major cause of tissue disruption. J Trauma 24(1):35–39

3. Fackler ML, Surinchak JS, Malinowski JA, Bowen RE (1984) Wounding potential of the Russian AK-74 assault rifle. J Trauma 24(3):263–266

4. Fackler ML, Malinowski JA (1988) Ordnance gelatin for ballistic studies. Detrimental effect of excess heat used in gelatin preparation. Am J Forensic Med Pathol 9(3):218–219

5. Jussila J (2004) Preparing ballistic gelatine—review and proposal for a standard method. Forensic Sci Int 141(2–3):91–98

6. Jussila J (2005) Measurement of kinetic energy dissipation with gelatine fissure formation with special reference to gelatine validation. Forensic Sci Int 150(1):53–62

7. Gawlick H, Knappworst J (1975) Zielballistische Untersuchungsmethoden an Jagdbüchsengeschossen, Ballistisches Laboratorium für Munition der Dynamit. Nobel AG, Werk Stadeln

8. Ragsdale BD, Josselson A (1988) Predicting temporary cavity size from radial fissure measurements in ordnance gelatin. J Trauma 28(1 Suppl):S5–S9

9. Fackler ML, Malinowski JA (1985) The wound profile: a visual method for quantifying gunshot wound components, J. Trauma 25(6):522–529

10. Schyma CW (2010) Colour contrast in ballistic gelatine. Forensic Sci Int 197(1-3):114–118

11. Schyma C, Madea B (2012) Evaluation of the temporary cavity in ordnance gelatine. Forensic Sci Int 214(1–3):82–87

12. Schyma C, Brünig J, Jackowski C, Müller R (2017) Messung der Geschossgeschwindigkeit mittels Hochgeschwindigkeitskamera. Rechtsmedizin 27:273–277. https://doi.org/10.1007/s00194-017-0180-z

13. Schyma C, Infanger C, Müller R, Bauer K, Brünig J (2019) The deceleration of bullets in gelatine - a study based on high-speed video analysis. Forensic Sci Int 296:85–90. https://doi.org/10.1016/j.forsciint.2019.01.017

14. Schyma C, Bauer K, Brünig J (2017) The reference cube: a new ballistic model to generate staining in firearm barrels. Forensic Sci Med Pathol 13(2):188–195. https://doi.org/10.1007/s12024-017-9868-3

15. Schyma C, Herr N, Brünig J, Brenčičová E, Müller R (2017) The influence of the counterfort while ballistic testing using gelatine blocks. Int J Legal Med 131(5):1325–1332. https://doi.org/10.1007/s00414-017-1623-5

16. Kneubuehl BP, Glardon MJ (2010) Polizeigeschosse und ihre Deformation, Abhängigkeit von Geschwindigkeit und Schussdistanz. Rechtsmedizin 20:80–84. https://doi.org/10.1007/s00194-010-0658-4

17. Zhang J, Yoganandan N, Pintar FA, Guan Y, Gennarelli TA (2007) Experimental model for civilian ballistic brain injury biomechanics quantification. J Biomech 40(10):2341–2346

18. Schyma C (2012) Wounding capacity of muzzle-gas pressure. Int J Legal Med 126(3):371–376

19. Schyma C, Greschus S, Urbach H, Madea B (2012) Combined radio-colour contrast in the examination of ballistic head models. Int J Legal Med 126(4):607–613

20. Schyma C, Müller R, Brenčičová E, Brünig J (2018) Distortion of the temporary cavity and its influence on staining in firearm barrels. Forensic Sci Med Pathol 14(2):202–208. https://doi.org/10.1007/s12024-018-9971-0

21. Ragsdale BD, Josselson AR (1986) Winchester Silvertip® ammunition – a study in ordnance gelatin. J Forensic Sci 31(3):855–868

22. Lazarjan MS, Geoghegan PH, Jermy MC, Taylor M (2014) Experimental investigation of the mechanical properties of brain simulants used for cranial gunshot simulation. Forensic Sci Int 239:73–78

23. Falland-Cheung L, Waddell JN, Lazarjan MS, Jermy MC, Winter T, Tong D, Brunton PA (2017) Use of agar/glycerol and agar/glycerol/water as a translucent brain simulant for ballistic testing. J Mech Behav Biomed Mater 65:665–671. https://doi.org/10.1016/j.jmbbm.2016.09.034

24. Zhang L, Jackson WJ, Bentil SA (2019) The mechanical behavior of brain surrogates manufactured from silicone elastomers. J Mech Behav Biomed Mater 95:180–190. https://doi.org/10.1016/j.jmbbm.2019.04.005

25. Singh D, Boakye-Yiadom S, Cronin DS (2019) Comparison of porcine brain mechanical properties to potential tissue simulant materials in quasi-static and sinusoidal compression. J Biomech 92:84–91. https://doi.org/10.1016/j.jbiomech.2019.05.033